2009 IEEE International Conference on Robotics and Automation
Kobe International Conference Center
Kobe, Japan, May 12-17, 2009

Mechanical design of a novel Hand Exoskeleton for accurate force displaying

M.Fontana, A. Dettori, F. Salsedo and M.Bergamasco

Abstract— **This paper deals with the mechanical design of a novel haptic Hand Exoskeleton (HE) that allows exerting controlled forces on the fingertip of the index and thumb of the operator. The proposed device includes several design solutions for optimizing the accuracy and mechanical performances. Remote Centers of Motion mechanisms have been adopted for delocalizing the encumbrance of linkages of the structure away from the operator's fingers. An improved stiffness of the transmission and reduced requirements for the actuators have been achieved thanks to a novel Patent Pending principle for integrating speed reduction ratio with the transmission system.**

I. Introduction

An Exoskeletric Haptic Interface (EHI) is a haptic device whose mechanical structure is located in proximity of the part of the body that is interested in the interaction. The kinematics of such devices is often designed in a way that the linkages of the structure follow the movements of the human operator. EHIs have attracted a lot of attention among the haptic research community since they show several advantages. Their most relevant feature is the optimal workspace matching between the human reachable workspace and the haptic device workspace. Moreover, EHIs perfectly fit the application where reduced visual and spatial encumbrance is needed.

Hand Exoskeletons (HE) belongs to the family of EHI. Their functionality is to exert controlled forces on the human fingers. HE can be classified in two functional sub-categories depending on the capability of exerting forces on one phalanx only (the fingertip) or on multiple phalanxes.

Mutli-Phalanx Hand Exoskeletons (MPHE) are devices able to exert different forces on more than one of the phalanxes of the same finger (see Fig. 1 on the left); commonly the force can be applied on a fixed direction normal to the phalanx axis and belonging to the medial plane of the finger. Single-Phalanx Hand Exoskeletons (SPHE): are able to exert forces on the distal phalanx only; some devices are able to generate a force only along a fixed direction but more commonly they can exert forces along any wanted direction (see Fig 1on the right).

HE can be further distinguished in two other categories:

- Anthropomorphic Device: when the kinematic of the HE is morphologically similar to the kinematic of the fingers;
- Non-anthropomorphic: when the kinematic of the HE is morphologically different from the finger scheme.

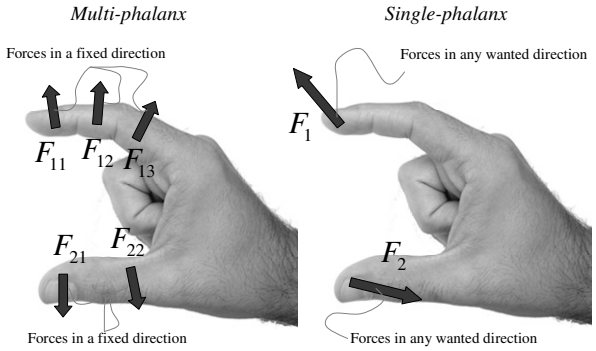

Fig.1: Multi-Phalanx and Single phalanx scheme

In the scientific literature of the last 30 years there are many works reporting the design of different HEs. The first example of HE was introduced by Zarudiansky back in 1981 [1]. The inventor has registered a patent on a telemanipulation system equipped with a master device able to provide force feedback on different phalanxes of the human hand. At JPL laboratory, in 1988, Jau [2] built a complete teleoperated master/slave arm comprehending a hand exoskeleton device for four fingers. In the same years Burdea develops a pneumatic actuated hand force feedback device [3] able to exert a single force on the distal phalanx along a direction that is assigned by the kinematic of the device and the position of the finger.

Few years later, Bergamasco [4] et al., at PERCRO Laboratory, developed another four fingers MPHE able to exert forces on each phalanx of each finger. A non-isomorphic device was realized by Koyama from Keio University. The device is a three finger exoskeleton with passive clutches actuation [5]; the device that is anchored on the wrist of the user and it is able to exert forces in every direction belonging to the sagittal plane of the fingers. Frisoli in [6] developed another non-isomorphic HE called Pure Form Hand-Exos for VR applications.

Nakagawara [7] built a device integrating the concept of encountered haptics in the field of exoskeletons. The device is a HE with just 1 DoF for each finger and it is able to track the finger of the user without any contact (even at the fingertip) through a non contact sensor placed in correspondence of the nail. When the contact takes place in

Manuscript received September 15, 2008. This work was supported in part by the European Project HAPTEX.

M.Fontana, F. Salsedo and M. Bergamasco are with PERCRO Laboratory, Scuola Superiore Sant'Anna, Pisa, Italy, +39050883059; fax: +39050883333; e-mail: [m.fontana, f.salsedo, m.bergamasco]@sssup.it.

the remote environment a plate is moved against the user fingertip.

In this paper we describe the design procedure of a high performance portable HE able to exert forces in the range of few Newtons but with exceptional capabilities of accuracy and resolution. The target of application of the HE that is described in this paper is the haptic interaction in virtual environment or in tele-manipulation systems. The reference tasks are the precision grasping between index and thumb, the manipulation and the exploration of surfaces and objects involving forces in the range of 0-5N.

The realized device (shown in Fig. 2) is able to exert controlled forces on any wanted direction on the two fingertips of the index and thumb of the right hand of the operator. The design work aimed at the realization of a high performance device able to render light forces in an accurate way. For the achievement of such performances some novel mechanical solutions has been conceived.

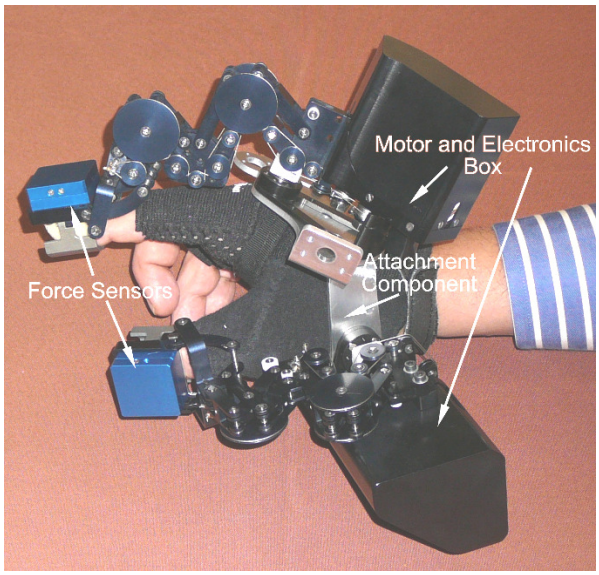

Fig. 2: Picture of the assembly of the realized Hand Exoskeleton

II. KINEMATICS

A. Architecture

The kinematic scheme that has been adopted for the developed HE can be defined as a *quasi-anthropomorphic* kinematics. The choice was driven by the fact that anthropomorphic kinematics presents many positive features that well fit the requirements of a portable haptic devices:

- Highest matching ratio between workspace of the mechanism and required workspace
- Short path for the robotic linkages
- Wearability with limited visual encumbrance

Anthropomorphic kinematics is usually adopted for MPHE since the links of the device have to accurately follow the movements of the phalanxes. Differently, in our design, we adopt a kinematics that is morphologically identical to finger kinematics but it slightly differs for the length of the links. The perfect coincidence would be desirable but it is not allowed because when the flexion joints of the finger are extended the kinematics falls in a singularity position.

The concept of *quasi-anthropomorphic* kinematics is represented in Fig.3. The finger kinematic model that has been taken as reference is the one adopted by Springer in [8]. Such model considers both the index and thumb finger as 4 DoFs 4R manipulator.

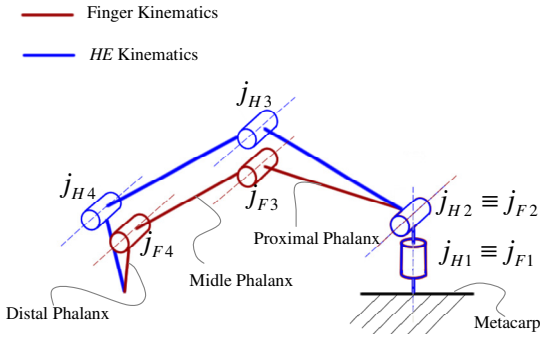

Fig. 3: Scheme of the kinematics of the HE

A simplification has been assumed for reducing the needed number of actuators. The actuation of 4 DoFs would require the use of 4 actuators and, since the actuators generally constitute the heaviest fraction of the mechanical assembly of an HI, we introduce a simplification that allows the use of only 3 motors. The rotation between the distal and middle phalanx (joint j_{H4}) has been coupled with the rotation between the middle and the proximal phalanx (joint j_{H3}). This coupling reflects the behavior of the human finger and in particular it has been assumed that the rotation of the joint j_{F4} is equal to the rotation of the joint j_{F3}. The implementation of such feature has been realized through a custom designed mechanism that is described in the following section.

B. Kinematics implementation

In Fig.4 the implementation of the whole kinematics is shown.

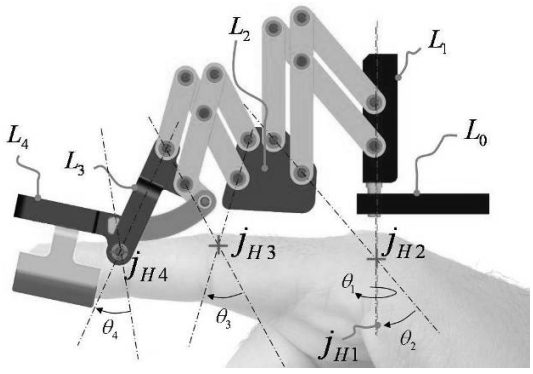

Fig.4: Implementation of the kinematics

1) Ab/ad-duction joint : j_{H1}

The first joint (j_{H1} in Fig.4) of the kinematic chain was implemented through a bearing joint whose encumbrance is located on the dorsal side of the palm of the hand. The axis has been oriented along the normal to the plane containing the hand palm.

2) Flexion-extension joint: j_{H2} and j_{H3} :

A critical aspect for the design of the flexion-extension joints j_{H2} and j_{H3} is to consider that collisions can occur between the links and finger of the user. A possible solution is to use bearing joints located at the side of the finger like proposed in [9]. In this solution, the joints with their bearings are located on both the sides of the finger. This implementation is functional and reliable but clearly shows the drawback of the lateral encumbrance of the joints that impedes two fingers to come near each other.

The implementation that we adopted makes use of *Remote Center of Motion* (RCM) systems. RCM are mechanisms that are able to implement the rotation of a body around a fixed axis that is remotely located from the structure of the joint. There are several mechanisms able to implement this feature. Many of them are reported and analyzed by Pei [10] and Fiaschi [11]. Fiaschi has analyzed several RCM for the implementation of flexion joints of HEs. The analysis consists of a score ranking that considers the complexity of implementation, the encumbrance and the mechanical characteristics. The simple RCM composed by two parallelograms connected together to form a 6-bar mechanism as in Fig.5 resulted the best ranked. Such mechanism allows the *Link i* to rotate around the Remote Center of Rotation (RCR).

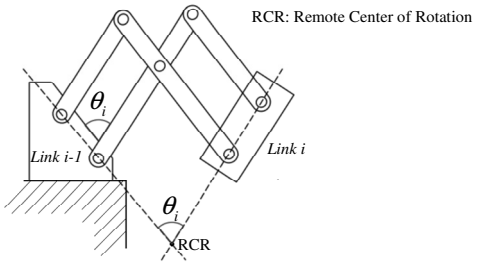

Fig. 5: Scheme of the Remote Center of Motion

Such RCM was chosen for the implementation of the flexion joint of the developed HE allowing to locate all the encumbrance mechanism of the HE in the dorsal side of the finger.

3) Distal Joint : j_{H4}

The j_{H4} could have been implemented with RCM as well. However the choice was to use lateral bearings solution. The choice was commanded by the need of leaving the dorsal side of the last link free to host a tactile array that will be added in the next future.

As mentioned in the previous section the joint j_{H4} has to be coupled with the rotation of the joint j_{H3}.

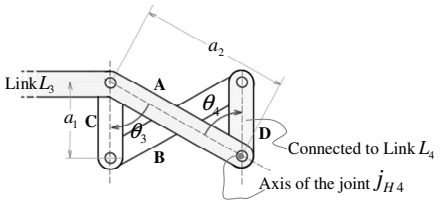

Fig. 6: Implementation of the joint j_{H4} with a crossed parallelogram

The coupling between the joints j_{H4} and j_{H3} has been implemented through a crossed parallelogram mechanism like the one depicted in Fig.6. The link A is rigidly connected to the link L_3 of the HE and the link D is connected to the link L_4. The rotation θ_3 is rotation between the links L_3 and L_2 and it is taken as input rotation for the crossed parallelogram mechanism. The axis of rotation of the link D coincides with the axis of the joint j_{H4} of Fig.4.

The ratio between the angular velocity of the link D (output) respect to the angular rotation of the link C (input) can be expressed with the following formula:

$$\gamma = \frac{\dot{\theta}_4}{\dot{\theta}_3} = 2\left(\frac{1+\delta\cos\theta_3}{1-\delta^2}\right) - 1$$

where:

$$\delta = \frac{a_1}{a_2}$$

As previously anticipated the ratio between the rotation of the distal respect to the medial phalanx and the rotation of the medial respect to the proximal phalanx of the human finger is approximately constant and unitary. So it would be desirable to have a $\gamma \cong 1$ for every value of θ_3. In Fig.7 the ratio γ is plotted in function of the angle θ_3. The different curves are referred to different values of δ. As it can be observed in figure when δ assumes small values the transmission ratio tends to one. On the other hand, small values δ cause overload on the leverage of the crossed parallelogram. A value of $\delta = 0.2$ was chosen as compromise.

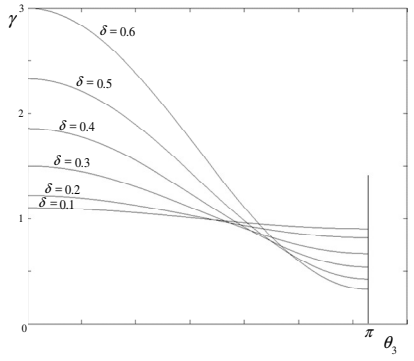

Fig. 7: Ratio between the rotation of the joints j_{H4} and j_{H3}

III. FORCE TRANSMISSION AND ACTUATION

The weight of the actuators is usually the largest fraction of the global weight of an HI so their placement has to be carefully considered by designing a proper force transmission system.

For the devices based on a serial kinematics scheme, the actuators are rarely placed directly on the joint axes because of the waste of motor torque for gravity compensation. A common approach is to delocalize the motors from the linkage structure placing them on the base of the mechanism using steel cable transmission for transmitting the torques. This has been the choice for many haptic interface designers like in [12] and [13].

In the design of the presented HE the choice was to locate the motors on the first link $\boldsymbol{L_1}$ of the mechanism as represented in Fig.8. This solution allows to largely simplify the routing of the cables for the actuation of the joints $\boldsymbol{j_{H2}}$ and $\boldsymbol{j_{H3}}$. Actually, the kinematic structure seen from a reference system that moves with the link $\boldsymbol{L_1}$ is a 3R planar kinematics mechanism.

The joint $\boldsymbol{j_1}$ is actuated through a classical capstan-pulley transmission (represented in Fig. 8). This implementation includes the use of a double cable transmission, i.e. a cable for driving the abduction and a different cable for the adduction.

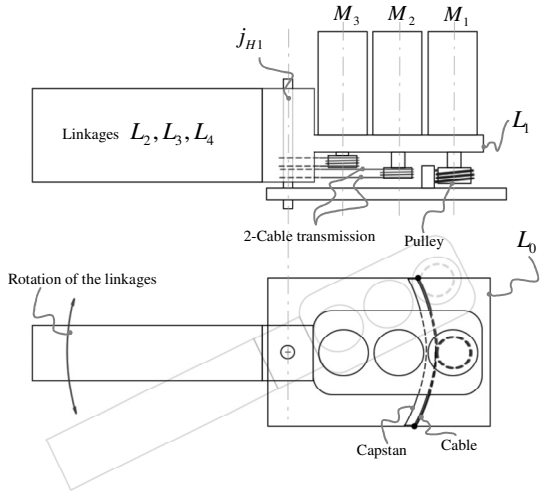

Fig. 8: Motor location and routing of transmission for the joint $\boldsymbol{j_{H1}}$

Such transmission presents the positive feature of introducing a structural speed reduction with very low friction forces. The speed reduction ratio value is:

$$r_{11} = \frac{R_{m1}}{R_c}$$

where:

R_c : radius of the capstan

R_{m1} : radius of the pulley of the motor 1

A different solution has been considered, for the actuation of the RCM that implements the flexion joint. The simple use of a capstan-pulley transmission (see Fig. 9) in this case is not suitable. The main drawback of this solution is that the radius of the driven pulley (R_1) has to be very large in order to reach a consistent speed reduction ratio.

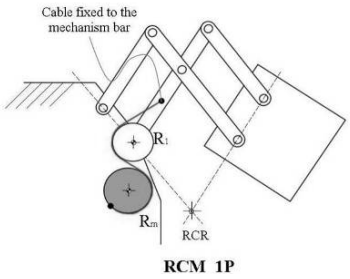

Fig. 9: Example of actuation for the RCM

For this reason a novel method for actuating the RCM has been conceived. The idea was to exploit the mutual rotation of the various links of the RCM structure in order to multiply the length change of the cable while the mechanism rotates. The implementation of this idea is achieved adding multiple idle pulleys coaxial with the rotation axes of the RCM and arranging the cables path beginning from the motor pulley, wrapping around the different idle pulleys and ending on attachment point on a link. Some variants of such kind of transmission system are represented in Fig.10. It can be shown that this transmission implements an intrinsic speed reduction ratio. The speed reduction can be found calculating the rotation of the motor pulley that corresponds to a given rotation of the joint. In particular, when the joint rotates in counter clockwise direction the change of length of the cable path is equal the sum of the changes of length of each cable segment that is wrapped around each pulley.

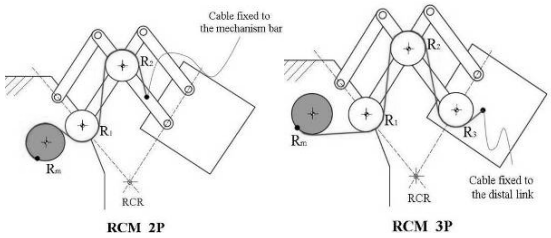

Fig.10: Different examples of transmission for RCM

From these considerations the speed reduction ratio can be computed as:

$$r = \frac{R_m}{\sum_{i=1}^{n} R_i} = \frac{R_m}{R_{eq}} \qquad (1)$$

where:

R_i : is the radius of pulley i ;

R_m : is the radius of the motor pulley

R_{eq} : radius of the capstan that has to be used for

achieving the same speed reduction.

The mechanisms can be seen as a capstan pulley system where the radius of the pulley (R_{eq}) is the sum of the radius of the idle pulley. The main advantage of this solution is that the global encumbrance of the mechanism is consistently reduced.

The complete transmission that includes the flexion and extension cables is represented for the joint j_{H2} in Fig.11.

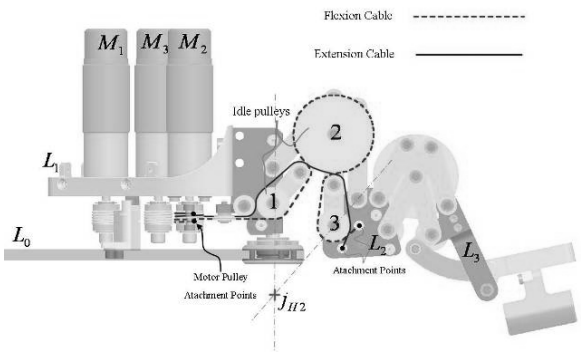

Fig. 11: Scheme of the transmission routing for the joint j_{H2}

The dotted line represents the path of the flexion cable and the solid line the extension one. The cables are routed on two parallel planes on two paths thanks to a double slot applied on each pulley. All the pulleys are idle and the cables are only fixed at the motor pulley and at the link L_2 through a crimp-slot attachment (indicated in the picture as "attachment points").

As previously anticipated the interesting feature of this kind of transmission is the implementation of an intrinsic speed reduction ratio between the rotation of the pulley of the motor M_2 and the joint j_{H2}.

The ratio can be easily calculated through the equation (1) considering the three idle pulleys 1, 2 and 3 and the motor pulley R_m. With the chosen dimensions a reduction ratio of about *1:5* is achieved.

The transmission for the joint j_{H3} is located on the other side of the assembly (see Fig.12). In this case scheme is more complex since the cables have to go through the joint j_{H2}. The cables run along the same path of the first transmission through the joint j_{H2} and follow an analogous routing scheme for the joint j_{H3}.

The speed reduction (r_{33}) is computed with the equation (1) considering the radius of the pulleys 4, 5 and 6 in Fig.12.

It is also important to consider that the rotation of the motor M_3 is also function of the rotation of the joint j_{H2}. The ratio between the rotation of the join j_{H2} and the rotation of pulley of the motor M_3 when the joint j_{H3} is blocked is indicated with r_{23} and can be computed with the formula (1) considering the radius of the pulley 7, 8 and 9.

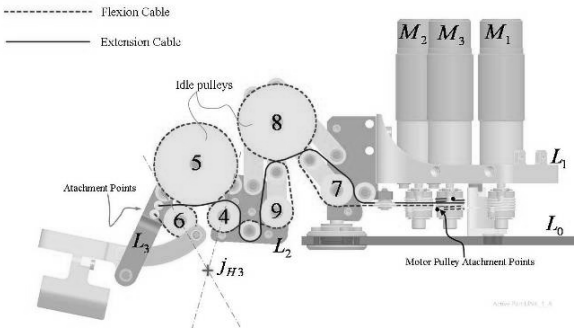

Fig.12: Scheme of the transmission routing for the joint j_{H3}

The relation between the joints velocities and the motor axes velocities can be expressed as follows:

$$\underset{\sim}{\dot{\theta}}_m = \begin{bmatrix} r_{11} & 0 & 0 \\ 0 & r_{22} & 0 \\ 0 & r_{23} & r_{33} \end{bmatrix} \underset{\sim}{\dot{\theta}}_j = T \underset{\sim}{\dot{\theta}}_j \qquad (2)$$

where:

$\underset{\sim}{\dot{\theta}}_m$: is the vector of the rotation speed of the motor pulleys

$\underset{\sim}{\dot{\theta}}_j$: is the vector of the rotation speed of the joints

The introduction of a speed reduction ratio intrinsically implemented in the transmission system introduces two advantages. Firstly for a given wanted maximum force at the end-effector, the size of the motors can be reduced consequently reducing the weight and encumbrance. Secondly the stiffness of the transmission is increased since the cable is less loaded. Moreover here it will be show that the resulting triangular form for the transmission matrix of equation (2) can be exploited for a further reducing the actuators requirements.

The force at the end-effector of the mechanism can be calculated as:

$$f = J_H^{-T} T^T \tau_m$$

Indicating with

J_H : is the Jacobian matrix and it establishes the relation between the end-effector velocity and the joint velocity expressed in the coordinate frame of the first link L_1

τ_m : the vector of the torques applied at the motor axis

For dimensioning the required torque it is useful to look at the maximum torque at the motor axis when a unit force of 1N is applied in every direction at the end-effector:

$$f^T f = 1$$

In the space of the motor torque variables the image of this sphere is an ellipsoid of equation:

$$\tau_m A \tau_m = 1$$

the matrix *A* assumes a particular form if expressed in the framework were the z-axis is aligned with the joint j_2 and

the x-axis belongs to the plane of the planar mechanism:

$$A = T\left(J_H J_H^T\right)^{-1} T^T = \begin{bmatrix} a_{11} & 0 & 0 \\ 0 & a_{22} & a_x \\ 0 & a_x & a_{33} \end{bmatrix}$$

The maximum torque at each motor *i* for a given point can be found maximizing the Lagrangian:

$$\zeta_i(p) = \tau_{m,i} + \lambda_i\left(\tau_m^T A \tau_m - 1\right)$$

For the given form of A the solutions can be computed:

$$\begin{cases} \overline{\tau}_{m,1(\theta_2,\theta_3)} = \sqrt{a_{11}} \\ \overline{\tau}_{m,2(\theta_3)} = \sqrt{\dfrac{a_{33}}{a_{22}\, a_{33} - a_x^2}} \\ \overline{\tau}_{m,3(\theta_3)} = \sqrt{\dfrac{a_{22}}{a_{22}\, a_{33} - a_x^2}} \end{cases}$$

The maximum torque $\overline{\tau}_{m,1}$ is function of θ_2 and θ_3 since it varies with the distance of the end-effector from the axis of the joint-1, while The torques $\overline{\tau}_{m,2}$ and $\overline{\tau}_{m,3}$ are function of only θ_3.

It's interesting to notice how the introduction of transmission matrix T reduces torque requirements for the joint j_{H2}. In Fig.13 (a) the values of the torque $\overline{\tau}_{m,2}$ and $\overline{\tau}_{m,3}$ when θ_3 varies from 0 to π and in Fig.13 (b) the values of $\overline{\tau}_{m,3}$ and $\overline{\tau}_{mnt,3}$ and considering a transmission with no-coupling – i.e. a diagonal T matrix.

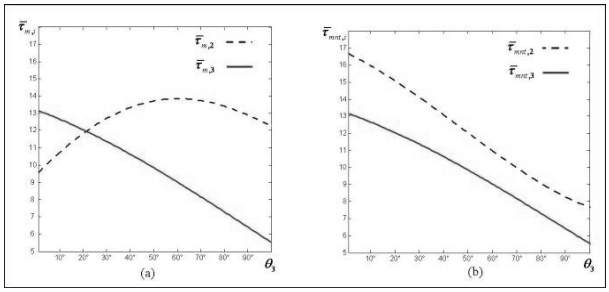

Fig. 13: Torque at the motor in function of the rotation of the second flexion angle in the case of triangular matrix (a) and non-triangular matrix (b).

IV. CONCLUSIONS

In this paper we have shown the mechanical design of a novel Hand Exoskeleton conceived for virtual reality and teleoperation purposes. The main mechanical solutions for optimizing the performance of the device consist of an improved implementation of the kinematic structure and a novel patented transmission system. It as been shown as these choices can positively influence the mechanical behaviour and the performances of the device.

A prototype of the device has been realized, Table I is a preliminary table of the main mechanical performance and in the next future it is foreseen to perform a mechanical characterization of the device and to design an optimized controller.

TABLE I
MAIN MECHANICAL PERFORMANCES

Symbol	Quantity	Value
DoF	Degrees of Freedom for each finger	3
F_{max}	Maximum continuous force	5N
W	Weight of the whole device	1.1 kg
w_a	Weight of one finger mechanism	0.51 kg
B_w	Mechanical Bandwidth (expected)	25 Hz

REFERENCES

[1] Zarudiansky, A., "Remote handling devices", United States Patents Archive, Pat. N.4302138.

[2] Jau B.M., Anthropomorphic exoskeleton dual arm/hand telerobot controller, IEEE International Workshop on Intelligent Robots, pp.715-718, 1988.

[3] Burdea G., J. Zhuang, E. Roskos, D. Silver and N. Langrana."'A portable dextrous master with force feedback", Presence: Teleoperators and Virtual Environments, Vol. l(l), pp. 18-28., 1992.

[4] Bergamasco, M., "Design of hand force feedback systems for glove-like advanced interfaces," Robot and Human Communication, 1992. Proceedings., IEEE International Workshop on , vol., no., pp.286-293, 1-3 Sep 1992.

[5] Koyama, T.; Yamano, I.; Takemura, K.; Maeno, T., "Multi-fingered exoskeleton haptic device using passive force feedback for dexterous teleoperation," Intelligent Robots and System, 2002. IEEE/RSJ International Conference on , vol.3, no., pp. 2905-2910 vol.3, 2002.

[6] Frisoli, A., Simoncini, F., Bergamasco, M. and Salsedo, F., "Kinematic Design of a Two Contact Points Haptic Interface for the Thumb and Index Fingers of the Hand", ASME J. Mech. Design, 129 (2007), 520-529.

[7] Nakagawara, S.; Kajimoto, H.; Kawakami, N.; Tachi, S.; Kawabuchi, I., "An Encounter-Type Multi-Fingered Master Hand Using Circuitous Joints," Robotics and Automation, 2005. ICRA 2005. Proceedings of the 2005 IEEE International Conference on , vol., no., pp. 2667-2672, 18-22 April 2005.

[8] Springer, S. and Ferrier, N.J. "Design and control of a force-reflecting haptic interface for teleoperational grasping"", ASME Journal of Mechanical Design, 1999

[9] Avizzano, C. A.; Barbagli, F.; Frisoli, A.; Bergamasco, M.: "The Hand Force Feedback: Analysis and Control of a Haptic Device for the Human Hand", Proc. of IEEE SMC 2000, Intern. Conf. on Systems, Man and Cybernetics, Nashville (TN-USA).

[10] Pei X., Yu J., Bi S., Zong G., "Enumeration and Type Synthesis of One-DOF Remote-Center-of-Motion Mechanisms" 12th IFToMM World Congress, Besançon (France), June18-21, 2007.

[11] Fiaschi, M., Salsedo, F., Bergamasco, M., "Analysis and Design of an Hand Exoskeleton", Bachelor Thesis in Mechanical Engineer, University of Pisa, 2003

[12] Frisoli, A., Rocchi, F., Marcheschi, S., Dettori, A., Salsedo, F., and Bergamasco, M. 2005. A New Force-Feedback Arm Exoskeleton for Haptic Interaction in Virtual Environments. In Proceedings of the First Joint Eurohaptics Conference and Symposium on Haptic interfaces For Virtual Environment and Teleoperator Systems (March 18 - 20, 2005)

[13] Hayward, V., Choski, J., Lanvin, G., Ramstein, C. "Design and multi-objective optimization of a linkage for haptic device", Advances in Robot Kinematics , Kluwer Academics, Vol-1,.pp 352-359